

## **PROCESSING PARACETAMOL-5-NITROISOPHTHALIC ACID COCRYSTAL USING SUPERCRITICAL CO<sub>2</sub> AS AN ANTI-SOLVENT**

**RAYMOND R. TJANDRAWINATA<sup>1,2\*</sup>, STEVANUS HIENDRAWAN<sup>1</sup>, BAMBANG VERIANSYAH<sup>1</sup>**

<sup>1</sup>Dexa Laboratories of Biomolecular Sciences (DLBS), Industri Selatan V Block PP No. 7, Jababeka Industrial Estate II, Cikarang 17550, West Java, Indonesia, <sup>2</sup>Faculty of Biotechnology, Atma Jaya Catholic University of Indonesia, Jalan Raya Cisauk-Lapan No. 10, Tangerang 15345, Indonesia

Email: raymond@dexa-medica.com

*Received: 12 Jun 2019, Revised and Accepted: 25 Jul 2019*

### **ABSTRACT**

**Objective:** A new method of cocrystallization based on the use of supercritical carbon dioxide (CO<sub>2</sub>) as an anti-solvent was explored. In the present study, we investigate and analyze paracetamol (PCA)-5-nitroisophthalic acid (5NIP) cocrystal produced using supercritical anti-solvent (SAS) process.

**Methods:** PCA-5NIP cocrystals prepared by SAS cocrystallization were compared to those produced using traditional solvent evaporation by rapid evaporation (RE) process. The cocrystals produced were characterized using powder X-ray diffraction (PXRD), differential scanning calorimetry (DSC), thermogravimetric analysis (TGA), polarized light microscopy (PLM), Fourier Transform Infrared (FTIR) spectroscopy, particle size analysis and scanning electron microscopy (SEM).

**Results:** The products obtained from SAS and RE process exhibited identical PXRD spectra and were distinguishable from the individual compounds, indicating the formation of a new phase. DSC analysis revealed that PCA-5NIP cocrystals from each method possess similar melting point which lies between the melting points of the parent compounds. Cocrystal particles with a mean diameter of 4.66 μm were produced from SAS process, which was smaller than those produced by traditional solvent evaporation method with a mean diameter of 38.09 μm.

**Conclusion:** This study demonstrates the ability of SAS process to produce the submicron size of PCA-5NIP cocrystal with altered physicochemical properties in a single step process.

**Keywords:** 5-nitroisophthalic acid, Carbon dioxide, Cocrystal, Paracetamol, Supercritical anti-solvent

© 2019 The Authors. Published by Innovare Academic Sciences Pvt Ltd. This is an open access article under the CC BY license (<http://creativecommons.org/licenses/by/4.0/>)  
DOI: <http://dx.doi.org/10.22159/ijap.2019v11i5.34554>

### **INTRODUCTION**

Pharmaceutical cocrystals have gained increasing popularity in the past decade due to their potentials in tuning various pharmaceutically relevant physicochemical properties such as solubility, permeability, bioavailability, hygroscopicity, mechanical properties and stability of active pharmaceutical ingredients (APIs) without compromising their pharmaceutical activity [1-7]. Pharmaceutical cocrystals also create new opportunities for pharmaceutical companies to address the intellectual property and new patent of APIs with regards to extend their life cycle [8]. A guidance and regulatory classification for pharmaceutical cocrystals has recently been released by European Medicines Agency (EMA) and United States Food and Drug Administration (FDA) [9, 10]. In the 2018 'Regulatory Classification of Pharmaceutical Co-Crystals: Guidance for Industry', US FDA classified cocrystal as a crystalline material composed of two or more different molecules, typically APIs and cocrystal formers ("coformers"), in the same crystal lattice. According to the recent rules, cocrystal is considered as a drug polymorph rather than a new API and hence, the drug development and regulatory submissions are simplified [10].

Pharmaceutical cocrystals have been produced using several methods such as solution crystallization (e. g. solvent evaporation, slurry, cooling, antisolvent addition and reaction crystallization methods) [11-13] and mechanochemical approaches (e. g. neat and solvent drop grinding) [14, 15]. However, these traditional methods exhibited several disadvantages in cocrystals screening and scaling-up process. Solution-based methods often require a large number of organic solvents which is environmentally undesirable. Furthermore, there is a risk of crystallization of the single-component phase during crystallization process that may lead to partial or no cocrystal formation. In addition, remaining solvent residues may contaminate the product, and the production of mechanical stress and heat evolution during the grinding process can affect the thermal degradation of the components. Therefore, the

development of novel and better methods for the screening and production of cocrystals is highly desirable [16-18].

Supercritical fluid (SCF)-based processes have also been used in cocrystal production as an alternative method. Several studies have previously been done in the production of pharmaceutical cocrystals using SCF techniques [19-24]. Carbon dioxide (CO<sub>2</sub>) at supercritical condition is mainly used due to its relatively low critical temperature (31.1 °C) and pressure (73.8 bar), nontoxic, nonflammable, environmentally benign and inexpensive [25]. The low solubility of many pharmaceutical compounds in supercritical CO<sub>2</sub> makes CO<sub>2</sub> anti-solvent an ideal technique for crystallization. Two of the most common CO<sub>2</sub> anti-solvent techniques used for the crystallization of pharmaceuticals are supercritical anti-solvent (SAS) and gas anti-solvent (GAS). SAS technique is a single step process for simultaneous cocrystallization and micronization. This process is suitable for compounds that possess low solubility in SCF. In this process, a solution of an organic solvent is pumped through a nozzle into a chamber simultaneously with an SCF, which act as the anti-solvent. The particles are generated due to the supersaturation of solute within the solution droplet [26, 27]. Compared to traditional cocrystallization methods, SAS cocrystallization offers several advantages, which include a single step process and reduction of thermal and mechanical stress on API compared to grinding processes, and reduction of organic solvent uses and residual solvent content in cocrystal product compared to traditional solution-based method [28, 29]. In the previous work, we have successfully prepared pharmaceutical cocrystals between the drug paracetamol and coformer dipicolinic acid using SAS process [30]. In this work, we investigated the cocrystallization of paracetamol (PCA) and 5-nitroisophthalic acid (5NIP) by SAS process. The resulting cocrystal was analyzed and compared to cocrystal from traditional solvent evaporation process [5]. Solid-state characterization techniques which include powder X-ray diffraction (PXRD), differential scanning calorimetry (DSC), fourier transform infrared (FTIR) spectroscopy, laser diffractometry (LD),

polarized light microscopy (PLM) and scanning electron microscopy (SEM) were performed for characterization.

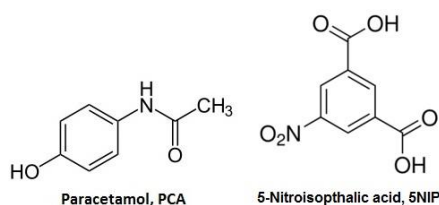


**Fig. 1: Chemical structure of paracetamol (PCA) and 5-nitroisophthalic acid (5NIP)**

## MATERIALS AND METHODS

### Materials

Paracetamol (PCA) was purchased from Zhejiang Kangle Pharmaceutical Co., Ltd. (Wenzhou, China). 5-Nitroisophthalic acid (5NIP) was obtained from Sigma-Aldrich, Co. (MO, USA). Methanol (ACS grade) was obtained from Merck KGaA (Darmstadt, Germany). High purity of carbon dioxide (CO<sub>2</sub>, purity of 99.95%) was purchased from PT Intergas (Jakarta, Indonesia). Polytetrafluoroethylene (PTFE) membrane with a size of 0.22 µm was purchased from Fioroni Filters (Ingre, France).

### Cocrystallization by the rapid evaporation process

Equimolar (1:1 mol ratio) quantities of PCA and 5NIP were dissolved in 20 ml of methanol and mixed under sonication at 40 °C for 10 min. The resulting solution was then placed into a crystallizing disk and heated at 70 °C for 5 h using a hot plate to evaporate the solvent. The dried solid was collected and placed in the glass vial for further analysis. The cocrystal product obtained from this experiment was further mentioned as PCA-5NIP-RE.

### SAS cocrystallization apparatus

Cocrystallization was conducted using a custom-built supercritical anti-solvent (SAS) apparatus as shown in fig. 2. Solution reservoir (9) was a 110 ml size Pyrex dropping funnel. High-pressure pump for CO<sub>2</sub> (3) was a Thar P-50 pump (Thar Technology, PA, USA). High-pressure pump for a solution (8) was a Lab Alliance 1200 series (Lab Alliance, PA, USA). The precipitation chamber (7) was made of stainless steel 316 (SS316) with 100 ml internal volume and water jacket to control the temperature of precipitator. To observe the process of particle formation, a pair of glass windows were installed in front and at the backside of precipitation chamber. A stainless steel capillary tube with internal diameter of 2.54 x 10<sup>-4</sup> m was used as a nozzle and it was placed on the top of precipitation chamber. The CO<sub>2</sub> precooler (2) and preheater (6) were a shell and tube type, respectively. The inner tube was a coiled tube with 0.6 m length and 3.175 x 10<sup>-3</sup> m outside diameter that made of SS316. The shell was made from SS316 with 0.11 m diameter and 0.25 m length. The products were filtered using 0.22 µm polytetrafluoroethylene (PTFE) membrane filter (10). Pressure of the precipitation chamber was controlled using a model 26-1721-24 back pressure regulator (11) manufactured by Tescom, Co. (MN, USA). The precooler and CO<sub>2</sub> pump temperature were maintained using a cooling circulator (4).

### SAS cocrystallization

Equimolar (1:1 mol ratio) quantities of PCA and 5NIP were dissolved in 20 ml of methanol and mixed under sonication at 40 °C for 10 min to obtain clear solution. The cocrystallization started by supplying fresh CO<sub>2</sub> into the precipitation chamber. After stable pressure (100 bar) and temperature (40 °C) was achieved, solution was sprayed into precipitation chamber at a flow rate of 1 ml/min and CO<sub>2</sub> was pumped into the precipitation chamber at the same time at a CO<sub>2</sub> flow rate of 30 g/min. After solutions have been sprayed, CO<sub>2</sub> was continuously supplied for 30 min to remove the remaining solvent in the product inside the precipitation chamber and filter. Products were collected from the filter after depressurizing the precipitation chamber. The cocrystal product obtained from this experiment was further mentioned as PCA-5NIP-SAS.

### Powder X-ray diffraction (PXRD)

Powder X-ray diffraction (PXRD) patterns were collected by Rigaku Ultima IV X-ray diffractometer (Rigaku Co., Tokyo, Japan) using Cu K $\alpha$  radiation ( $\lambda = 1.54 \text{ \AA}$ ), a tube voltage of 40 kV and a tube current of 40 mA. Data were collected from 2 to 40 ° at a continuous scan rate of 4 °/min.

### Differential scanning calorimetry (DSC)

Thermal analysis of the samples was performed using differential scanning calorimetry (DSC) on DSC Q20 (TA Instruments, DE, USA) which was calibrated for temperature and cell constants using indium. Samples (1-3 mg) crimped in the aluminum pan were analyzed from 50 to 300 °C with a heating rate of 10 °C/min. Samples were continuously purged with nitrogen at 50 ml/min.

### Thermogravimetric analysis (TGA)

Thermogravimetric analysis (TGA) was performed on a TGA Q50 (TA Instruments, DE, USA) instrument. Approximately 1-5 mg sample was heated from 50 to 300 °C in an open aluminum pan at a rate of 10 °C/min under nitrogen purge at a flow rate of 50 ml/min.

### Polarized light microscopy (PLM)

Polarized light microscopy (PLM) experiments were performed using BX-50 polarizing microscope (Olympus, Tokyo, Japan). Photomicrographs were captured using an Olympus SC-30 digital color camera and analyzed using AnalySIS getIT software.

### Fourier transform infrared (FTIR) spectroscopy

IR spectra of the compounds were recorded on an FT/IR-6100 type A infrared spectrometer (JASCO, MD, USA) in ATR mode from 4000-700 cm<sup>-1</sup> with a resolution of 4 cm<sup>-1</sup>.

### Particle size analysis

Particle size was determined by a laser diffractometer (Mastersizer 2000, Malvern Instruments, USA) using the dry powder dispersing system Scirocco 2000 at 2 bar pressure. Particle size was characterized by volume-weighted mean diameter D<sub>4,3</sub>. The particle size results represent the average values over three measurements performed on each sample.

### Scanning electron microscopy (SEM)

Morphology of the samples was analyzed using a JEOL JSM-6510 scanning electron microscopy (SEM, JEOL Ltd. Tokyo, Japan). Samples were mounted on a double-faced adhesive tape, sputtered with platinum. Scanning electron photographs were taken at an accelerating voltage of 5 kV.

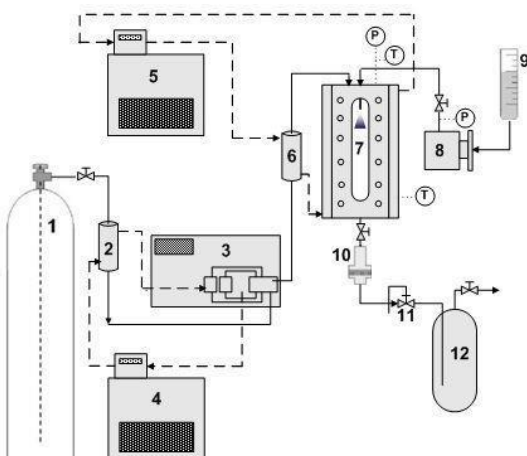


**Fig. 2: Schematic diagram of custom-built SAS apparatus: (1) CO<sub>2</sub> cylinder, (2) precooler, (3) high-pressure pump for CO<sub>2</sub>, (4) cooling bath, (5) heating bath, (6) preheater, (7) precipitation chamber, (8) high-pressure pump for solution, (9) solution reservoir, (10) filter, (11) back pressure regulator, (12) separator**

## RESULTS AND DISCUSSION

### Powder X-ray diffraction (PXRD) analysis

PXRD analysis was used to identify the formation of novel crystalline phase in solid-state. Every crystalline phase of a compound exhibited its own characteristic PXRD pattern, thus PXRD has commonly been used to distinguish the resulting products from the starting materials [5]. The PXRD patterns for PCA, 5NIP and PCA-5NIP physical mixture are shown in fig. 3a-c. PCA exhibited characteristic crystalline peaks at  $2\theta$  values of  $12.80^\circ$ ,  $15.50^\circ$ ,  $18.12^\circ$ ,  $21.96^\circ$ ,  $23.46^\circ$ ,  $24.34^\circ$  and  $26.50^\circ$ , whereas 5NIP exhibited characteristic crystalline peaks at  $2\theta$  values of  $18.00^\circ$ ,  $20.40^\circ$ ,  $21.14^\circ$ ,  $23.48^\circ$  and  $28.60^\circ$ . Fig. 3d-e shows PXRD patterns of the products obtained from cocrystallization process via rapid solvent evaporation and SAS. The products obtained from each method exhibited identical spectra, and the diffractogram of PCA-5NIP cocrystal was distinguishable from the individual compounds. The

different peaks in PXRD pattern of the cocrystal could imply the existence of interactions between PCA and 5NIP to form a new crystalline phase. This PXRD result also confirms that PCA-5NIP cocrystal was successfully produced from SAS cocrystallization experiment and exhibited similar internal crystal structure with PCA-5NIP cocrystal from rapid solvent evaporation process. As shown in fig. 3d-e, the intensity of the diffraction peaks were different at several  $2\theta$  positions, although the characteristic diffraction peaks from PCA-5NIP-RE and PCA-5NIP-SAS cocrystals were observed at the same  $2\theta$  position.

The difference of diffraction peaks intensity can be explained by the preferred orientation, which is a condition in which the distribution of crystal orientation is non-random and a specific crystalline frame may tend to cluster to a greater or lesser degree about some particular orientations [31]. These results showed that crystallization condition may control the crystallinity of the product.

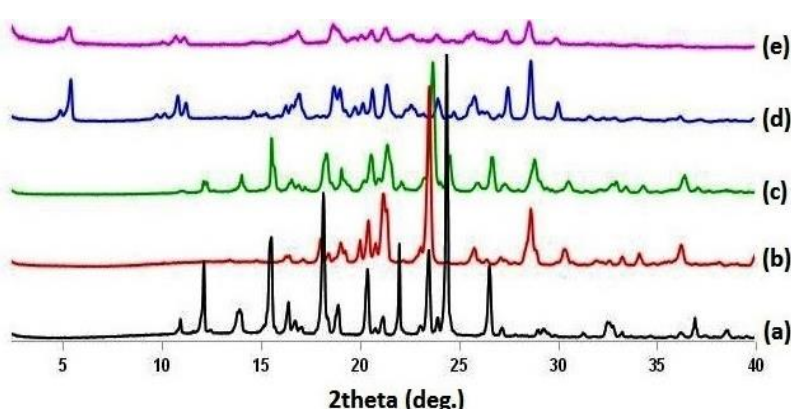


Fig. 3: Powder X-ray diffractograms of (a) PCA, (b) 5NIP, (c) physical mixture of PCA and 5NIP (1:1 mol ratio), (d) PCA-5NIP-RE and (e) PCA-5NIP-SAS

### Thermal analysis

DSC and TGA experiments were carried out to study the thermal behavior of PCA-5NIP cocrystals. DSC thermograph of PCA, 5NIP, physical mixture of PCA and 5NIP at 1:1 mol ratio, PCA-5NIP-RE and PCA-5NIP-SAS are shown in fig. 4. It shows that PCA exhibited a melting endothermic peak at  $170.23^\circ\text{C}$ , while 5NIP showed a melting endothermic at  $260.28^\circ\text{C}$ . DSC analysis of the physical mixture of PCA and 5NIP showed 4 endothermic peaks (fig. 4c). First endothermic peak at  $148.66^\circ\text{C}$  could be attributed to the eutectic temperature of PCA and 5NIP mixture, and second melting endotherm at  $162.69^\circ\text{C}$  was indicated as cocrystal eutectic melting with an excess of high-melting component. The third peak at  $204.11^\circ\text{C}$  indicates the melting point of the cocrystal followed by decomposition of cocrystal, as confirmed by TGA result. This observation was in accordance to the report by Lu *et al.* which demonstrated that DSC can be used for cocrystal screening [32]. They explained that the formation of cocrystal could be predicted if there were two endothermic peaks (corresponding to eutectic mixture and cocrystal melting) obtained during the physical mixture melting process in DSC analysis. DSC analysis of the products from cocrystallization experiments showed single endothermic peak which lies between the melting points of the parent compounds. PCA-5NIP-RE and PCA-5NIP-SAS exhibited endothermic melting point at  $205.28^\circ\text{C}$  and  $203.93^\circ\text{C}$ , respectively. A statistical study by Perlovich on 727 cocrystal systems indicated that the majority of cocrystals (55.3%) exhibited melting points in between those of the drug and coformer, while 15.8% of cocrystals possessed higher melting point and 28.9% showed lower melting point than those of the individual compounds [33]. The shift in the melting point of PCA-5NIP cocrystal might be attributable to the interaction between PCA and 5NIP, which altered the change in the crystal lattice and formed a relatively different internal crystal structure of PCA-5NIP cocrystal [34]. The enthalpy of fusion,  $\Delta H$  of PCA-5NIP-RE and PCA-5NIP-SAS

were 192.0 and 94.93 J/g, respectively, which showed that cocrystal from SAS cocrystallization possesses lower enthalpy of fusion. The lower enthalpy of fusion of PCA-5NIP cocrystal from SAS process might possibly due to the reduction of particle size or lowered crystallinity following SAS process [25, 35].

TGA was conducted to analyze the changes in cocrystal weight with regards to the change of temperature (fig. 5). TGA curve showed no weight loss until melting, suggesting that PCA-5NIP-RE and PCA-5NIP-SAS cocrystals were not solvated or hydrated. TGA of these cocrystals showed the occurrence of mass loss after melting points, which attributed to the degradation of cocrystals.

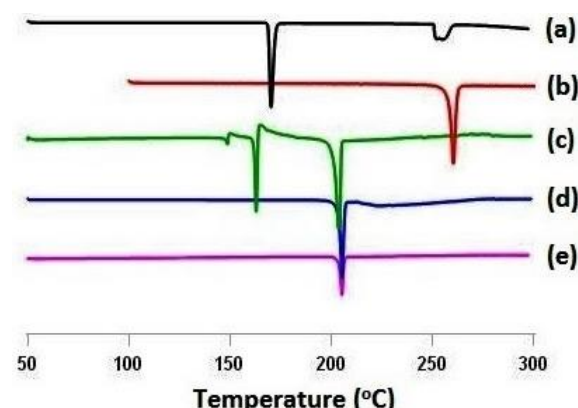


Fig. 4: DSC thermograms of (a) PCA, (b) 5NIP, (c) physical mixture of PCA: 5NIP (1:1 mol ratio), (d) PCA-5NIP-RE and (e) PCA-5NIP-SAS

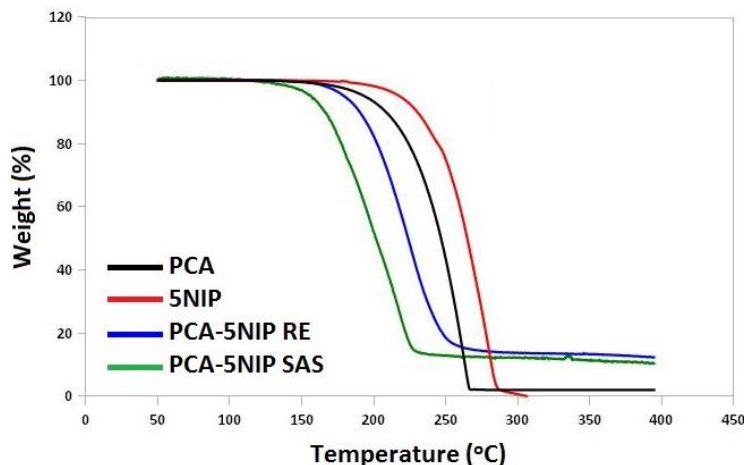


Fig. 5: TGA thermograms of PCA, 5NIP, PCA-5NIP-RE and PCA-5NIP-SAS

#### Fourier transform infrared (FTIR) spectroscopy

FTIR spectroscopy can be used to confirm cocrystal formation by evaluating the changes in vibrational frequencies of specific functional groups of the product compared to their starting components [36]. Based on the chemical structures of PCA and 5NIP (fig. 1), there are several functional groups that are able to form intermolecular hydrogen bonding, and thus several possible synthons to form can be obtained. The FTIR spectra of PCA, 5NIP, PCA-5NIP-RE and PCA-5NIP-SAS cocrystal are shown in fig. 6. FTIR

spectra of PCA-5NIP cocrystal showed several different wavenumbers for several major bands compared to their individual components. The new bands at 3446.42 cm<sup>-1</sup> in PCA-5NIP-RE cocrystals and 3465.46 cm<sup>-1</sup> in PCA-5NIP-SAS cocrystals can be assigned to the intermolecular hydrogen bond interaction between O carboxylic acid and N-H amide (O···N-H) [37, 38]. The shift in spectral peaks has also been observed for the carbonyl functional groups, indicating its participation in hydrogen bonding between cocrystal formers.

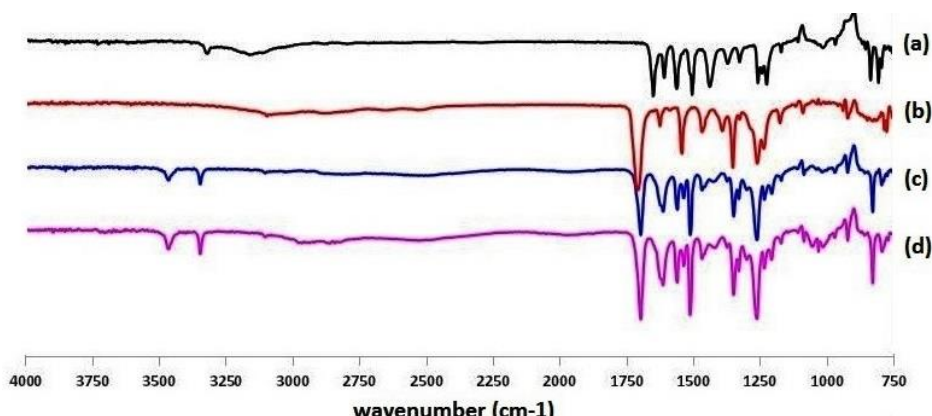


Fig. 6: FTIR spectra of (a) PCA, (b) 5NIP, (c) PCA-5NIP-RE and (d) PCA-5NIP-SAS

#### Polarized light microscope (PLM) images

Fig. 7 shows PLM photomicrographs of PCA, 5NIP and physical mixture of PCA and 5NIP (1:1 mol ratio) after recrystallization from methanol. It showed that recrystallization of PCA and 5NIP (1:1 mol ratio) physical mixture produced different crystal habit compared to the crystal habit of its starting components (PCA and 5NIP). Although in general, the different crystal habit between crystallization product and its starting components was not a proof to the formation of a new crystalline phase, this phenomena may provide a preliminary information about the possible interaction of the starting components to produce a new crystalline phase (cocrystal). In this study, the interaction between PCA and 5NIP produced a new crystalline phase as confirmed by PXRD, DSC and FTIR analysis, and thus we conclude that the different crystal habit was generated due to the interaction between PCA and 5NIP to form a new crystalline phase. Crystal habit of a drug is an important variable in pharmaceutical manufacturing. The changes in the crystal habit of a raw material after cocrystallization may influence its physico-mechanical properties and affect the performance of the dosage form [39].

#### Scanning electron microscope (SEM) and laser diffractometer (LD) analysis

Fig. 8 shows SEM micrographs of PCA, 5NIP, and PCA-5NIP cocrystal. PCA and 5NIP crystals exhibited an irregular rod-like or columnar habit, whereas PCA-5NIP-RE and PCA-5NIP-SAS cocrystal showed thin plate-like crystals. SEM micrographs of the cocrystal clearly show that the crystal habit of PCA-5NIP cocrystal was different compared to its individual components. SEM image also revealed that cocrystal from SAS process showed a smaller particle size compared to those produced from the rapid evaporation process. Crystal habit of the API is an important parameter in pharmaceutical processing, since it influences various pharmaceutical parameters such as flow properties and compaction characteristic of drug powder [39]. The particle size distribution (PSD) patterns from LD analysis illustrated in fig. 9 show that SAS process can produce PCA-5NIP cocrystal with smaller average particle size and narrower PSD. This result indicates that SAS process is an efficient process to produce sub-micron size of PCA-5NIP cocrystal.

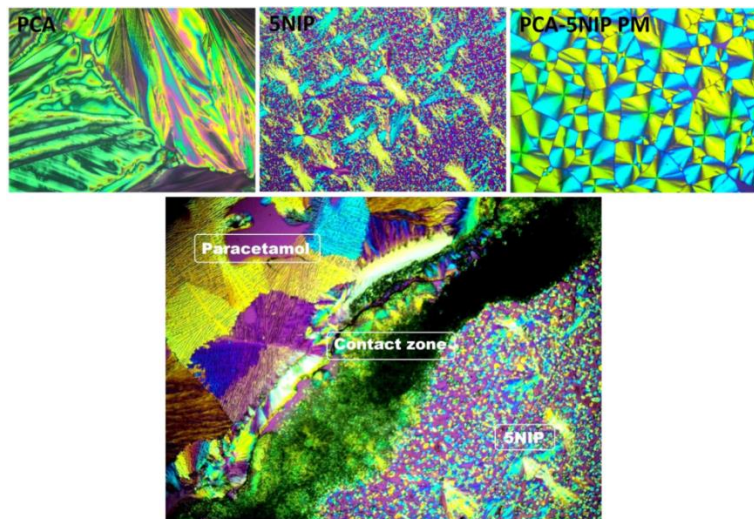


**Fig. 7:** Polarized light microscopy (PLM) images of PCA, 5NIP and physical mixture of PCA: 5NIP (1:1 mol ratio) after recrystallization using methanol (PM)

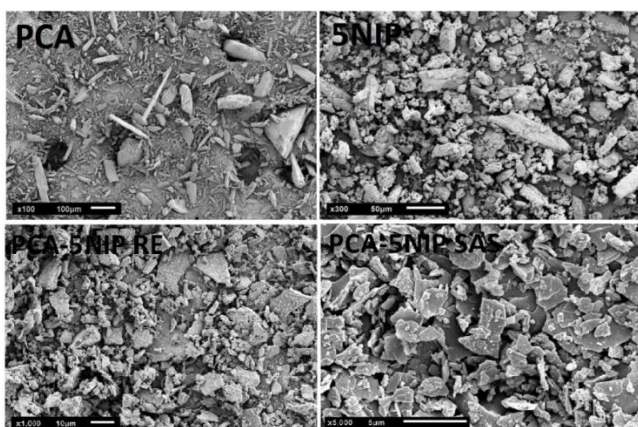


**Fig. 8:** SEM images of PCA, 5NIP, PCA-5NIP-RE and PCA-5NIP-SAS

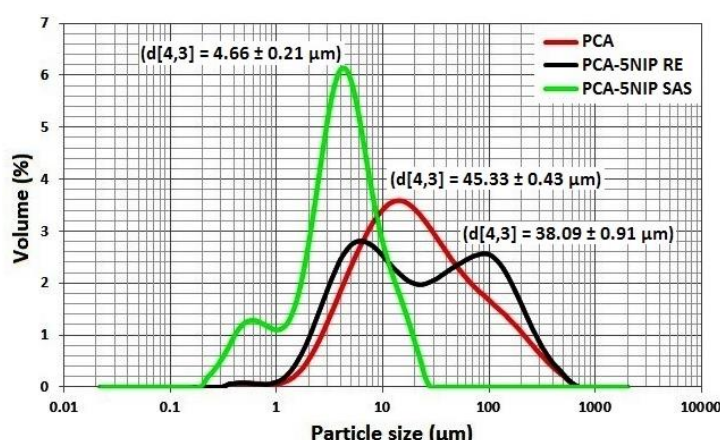


**Fig. 9:** Particle size distribution (PSD) profile of PCA, PCA-5NIP-RE and PCA-5NIP-SAS

## CONCLUSION

In summary, cocrystals of PCA and 5NIP were successfully prepared using supercritical anti-solvent (SAS) process. The formation of new crystalline phases was confirmed by PXRD, DSC, FTIR, PLM, SEM and LD analysis. Particle size of cocrystal particles produced by SAS was smaller than those produced by traditional rapid solvent evaporation process. This study demonstrates the ability of SAS

process to produce the sub-micron size of PCA-5NIP cocrystal with altered physicochemical properties in a single step process.

## ACKNOWLEDGMENT

The authors acknowledge Dexa Laboratories of Biomolecular Sciences (DLBS)-PT. Dexa Medica for financial support. The authors would like to thank Isabela Anjani for critical review on this manuscript.

**AUTHORS CONTRIBUTIONS**

All the author have contributed equally

**CONFLICT OF INTERESTS**

The authors declared no conflicts of interest with respect to the authorship and/or publication.

**REFERENCES**

1. Hiendrawan S, Hartanti AW, Veriansyah B, Widjojokusumo E, Tjandrawinata RR. Solubility enhancement of ketoconazole via salt and cocrystal formation. *Int J Pharm Pharm Sci* 2015;7:160-4.
2. Alatas F, Ratih H, Soewandhi SN. Enhancement of solubility and dissolution rate of telmisartan by telmisartan-oxalic acid co-crystal formation. *Int J Pharm Pharm Sci* 2015;7:423-6.
3. Fukte SR, Wagh MP, Rawat S. Coformer selection: an important tool in cocrystal formation. *Int J Pharm Pharm Sci* 2014;6:9-14.
4. Hiendrawan S, Veriansyah B, Tjandrawinata RR. Solid-state properties and solubility studies of a novel pharmaceutical cocrystal of Itraconazole. *Int J Appl Pharm* 2018;10:97-104.
5. Hiendrawan S, Veriansyah B, Widjojokusumo E, Soewandhi SN, Wikarsa S, Tjandrawinata RR. Physicochemical and mechanical properties of paracetamol cocrystal with 5-nitroisophthalic acid. *Int J Pharm* 2016;497:106-13.
6. Putra OD, Umeda D, Nugraha YP, Nango K, Yonemochi E, Uekusa H. Simultaneous improvement of epalrestat photostability and solubility via cocrystallization: a case study. *Cryst Growth Des* 2018;18:373-9.
7. Bolla G, Nangia A. Pharmaceutical cocrystals: walking the talk. *Chem Commun* 2016;52:8342-60.
8. Trask AV. An overview of pharmaceutical cocrystals as intellectual property. *Mol Pharm* 2007;4:301-9.
9. Reflection paper on the use of cocrystals and other solid-state forms of active substances in medicinal products. European Medicines Agency. Available from: [http://www.ema.europa.eu/docs/en\\_GB/document\\_library/Scientific\\_guideline/2015/07/WC500189927.pdf](http://www.ema.europa.eu/docs/en_GB/document_library/Scientific_guideline/2015/07/WC500189927.pdf). [Last accessed on 23 May 2019].
10. Guidance for industry: regulatory classification of pharmaceutical co-crystals. US Food and Drug Administration. Available from: <https://www.fda.gov/downloads/Drugs/Guidances/UCM281764.pdf>. [Last accessed on 23 May 2019].
11. Fucke K, Myz SA, Shakhtsneider TP, Boldyreva EV, Griesser UJ. How good are the crystallisation methods for co-crystals? A comparative study of piroxicam. *New J Chem* 2012;36:1969-77.
12. Takata N, Shiraki K, Takano R, Hayashi Y, Terada K. Cocrystal screening of stanalone and mestanalone using slurry crystallization. *Cryst Growth Des* 2008;88:3032-7.
13. Chen JM, Wang ZZ, Wu CB, Li S, Lu TB. Crystal engineering approach to improve the solubility of mebendazole. *Cryst Eng Comm* 2012;14:6221-9.
14. Trask AV, Jones W. Crystal engineering of organic cocrystals by the solid-state grinding approach. *Top Curr Chem* 2005;254:41-70.
15. Lin HL, Wu TK, Lin SY. Screening and characterization of cocrystal formation of metaxalone with short-chain dicarboxylic acids induced by solvent-assisted grinding approach. *Thermochim Acta* 2014;575:313-21.
16. Dhumal RS, Kelly AL, York P, Coates PD, Paradkar A. Cocrystallization and simultaneous agglomeration using hot melt extrusion. *Pharm Res* 2010;27:2725-33.
17. Patil SP, Modi SR, Bansal AK. Generation of 1:1 carbamazepine: nicotinamide cocrystals by spray drying. *Eur J Pharm Sci* 2014;62:251-7.
18. Eddleston MD, Patel B, Day GM, Jones W. Cocrystallization by freeze-drying: Preparation of novel multicomponent crystal forms. *Cryst Growth Des* 2013;13:4599-606.
19. Pando C, Cabanas A, Cuadra IA. Preparation of pharmaceutical co-crystals through sustainable processes using supercritical carbon dioxide: a review. *RSC Adv* 2016;6:71134-50.
20. Padrela L, Rodrigues MA, Velaga SP, Fernandes AC, Matos HA, de Azevedo EG. Screening for pharmaceutical cocrystals using the supercritical fluid enhanced atomization process. *J Supercrit Fluids* 2010;53:156-64.
21. Ober CA, Gupta RB. Formation of itraconazole-succinic acid cocrystals by gas antisolvent cocrystallization. *AAPS PharmSciTech* 2012;13:1396-406.
22. Mullers KC, Paisana M, Wahl MA. Simultaneous formation and micronization of pharmaceutical cocrystals by rapid expansion of supercritical solutions (RESS). *Pharm Res* 2015;32:702-13.
23. Zhao Z, Liu G, Lin Q, Jiang Y. Co-crystal of paracetamol and trimethylglycine prepared by a supercritical CO<sub>2</sub> anti-solvent process. *Chem Eng Technol* 2018;41:1-11.
24. Cuadra IA, Cabanas A, Cheda JAR, Pando C. Polymorphism in the co-crystallization of the anticonvulsant drug carbamazepine and saccharin using supercritical CO<sub>2</sub> as an anti-solvent. *J Supercrit Fluids* 2018;136:60-9.
25. Hiendrawan S, Veriansyah B, Tjandrawinata RR. Micronization of fenofibrate by rapid expansion of the supercritical solution. *J Ind Eng Chem* 2014;20:54-60.
26. Hiendrawan S, Veriansyah B, Widjojokusumo E, Tjandrawinata RR. Simultaneous micronization and purification of the bioactive fraction by supercritical antisolvent technology. *J Adv Pharm Technol Res* 2017;8:52-8.
27. Widjojokusumo E, Veriansyah B, Tjandrawinata RR. Supercritical anti-solvent (SAS) micronization of Manilkara kauki bioactive fraction (DLBS2347). *J CO<sub>2</sub> Util* 2013;4:30-6.
28. Ober CA, Montgomery SE, Gupta RB. Formation of itraconazole/l-malic acid cocrystals by gas antisolvent cocrystallization. *Powder Technol* 2013;236:122-31.
29. Neurohr C, Revelli AL, Billot P, Marchivie M, Lecomte S, Laugier S, et al. Naproxen-nicotinamide cocrystals produced by CO<sub>2</sub> antisolvent. *J Supercrit Fluids* 2013;83:78-85.
30. Hiendrawan S, Veriansyah B, Widjojokusumo E, Soewandhi SN, Wikarsa S, Tjandrawinata RR. Simultaneous cocrystallization and micronization of paracetamol-dipicolinic acid cocrystal by supercritical antisolvent (SAS). *Int J Pharm Pharm Sci* 2016;8:89-98.
31. Kim MS, Lee S, Park JS, Woo JS, Hwang SJ. Micronization of cilostazol using supercritical antisolvent (SAS) process: effect of process parameters. *Powder Technol* 2007;177:64-70.
32. Lu E, Hornedo NR, Suryanarayanan R. A rapid thermal method for cocrystal screening. *Cryst Eng Comm* 2008;10:665-8.
33. Perlovich GL. Thermodynamic characteristics of cocrystal formation and melting points for the rational design of pharmaceutical two-component systems. *Cryst Eng Comm* 2015;17:7019-28.
34. Bhandaru JS, Malothu N, Akkinapally RR. Characterization and solubility studies of pharmaceutical cocrystals of eprosartan mesylate. *Cryst Growth Des* 2015;15:1173-9.
35. Yeo SD, Lee JC. Crystallization of sulfamethizole using the supercritical and liquid antisolvent processes. *J Supercrit Fluids* 2004;30:315-23.
36. Chadha R, Saini A, Jain DS, Venugopalan P. Preparation and solid-state characterization of three novel multicomponent solid forms of oxcarbazepine: Improvement in solubility through saccharin cocrystal. *Cryst Growth Des* 2012;12:4211-24.
37. Chow SF, Shi L, Ng WW, Leung KHY, Nagapudi K, Sun CC, et al. Kinetic entrapment of a hidden curcumin cocrystal with phloroglucinol. *Cryst Growth Des* 2014;14:5079-89.
38. Wang L, Tan B, Zhang H, Deng Z. Pharmaceutical cocrystals of diflunisal with nicotinamide or iso-nicotinamide. *Org Process Res Dev* 2013;17:1413-8.
39. Garekani HA, Ford JL, Rubinstein MH, Siahboomi ARR. Formation and compression characteristics of prismatic polyhedral and thin plate-like crystals of paracetamol. *Int J Pharm* 1999;187:77-89.